J Mater Sci (2011) 46:3907–3913
DOI 10.1007/s10853-011-5314-1

Modeling and preparation of a super-oleophobic non-woven fabric

Hoon Joo Lee · Colin R. Willis · Corinne A. Stone

Received: 6 September 2010 / Accepted: 21 January 2011 / Published online: 8 February 2011

Abstract A super-oleophobic surface has been achieved by satisfying two conditions: a properly designed surface morphology and a low surface energy. A meta-stable Cassie–Baxter model has been used to account for the super-oleophobic effect with a truly random rough surface such as hydro-entangled non-woven fabric. In this model, a high contact angle is obtained by a minimum of surface energy due to air pockets inside the rough structure. Apparent dodecane contact angles of greater than 150° were measured on a hydro-entangled, non-woven nylon fabric whose fibers had been modified using a pulsed plasma discharge containing 1*H*,1*H*,2*H*,2*H*-perfluorodecylacrylate (PFAC8). Good agreement between the predicted and measured contact angles was obtained using the meta-stable Cassie–Baxter model.

Introduction

The phenomenon of super-repellency has been studied by the scientific community for a number of years [1–7]. One area of particular interest is the creation of artificial surfaces that mimic super-hydrophobic lotus leaves [8–12]. The ready shedding of water and dirt from such surfaces is commonly called the Lotus effect, although it is also observed on many other natural surfaces such as Lady's Mantle leaves, butterfly wings, duck feathers, and broccoli. It would be beneficial if similar materials with super-oleophobic properties existed, since the applications of such materials would be wide ranging [13].

A surface is called a super-hydrophobic surface if the water contact angle exceeds 150°. Similarly, we define a *super-oleophobic* surface as having an oil contact angle over 150°. In this context, "oil" refers to the non-polar alkane, dodecane. Although many researchers believe that the definition of a super-hydrophobic surface also requires a roll-off angle less than 5°, it is well known that the roll-off angles are strongly affected by the weight of a water droplet [14]. Hence, this study focuses on creating a super-oleophobic surface which has an oil contact angle greater than 150°, rather than dealing with a roll-off angle lower than 5°.

Since the wettability of a solid surface is determined by two parameters, surface energy and geometrical roughness, the combination of these two parameters can be used for the development of super-hydrophobic and super-oleophobic surfaces [15]. Two predominant wetting models are often used to describe wetting behavior of rough surfaces: the Wenzel model and the Cassie–Baxter model. In the Wenzel model, a liquid fills the grooves of a rough surface and completely wets the surface, whilst in the Cassie–Baxter model, a liquid sits on top of a composite surface consisting of a solid and air. In this approach the apparent contact angle on a Cassie–Baxter surface, θ_r^{CB}, can be described as:

$$\cos\theta_r^{CB} = f_1 \cos\theta_e - f_2 \quad (1)$$

where θ_e is the Young's contact angle on the corresponding flat surface, f_1 is the surface area of the liquid in contact with solid divided by the projected area, and f_2 is the surface area of the liquid in contact with air divided by the projected area [2]. If $f_2 = 0$ in Eq. 1, the liquid is in full

H. J. Lee (✉)
College of Textiles, North Carolina State University,
2401 Research Drive, Raleigh, NC 27695, USA
e-mail: hoonjoo_lee@ncsu.edu

C. R. Willis · C. A. Stone
Defence Science and Technology Laboratory (Dstl),
Porton Down, Salisbury, Wiltshire SP4 0JQ, UK

contact with the rough surface and completely wets it. This surface is therefore a Wenzel surface, and the apparent contact angle in Eq. 1, θ_r^{CB}, becomes an apparent contact angle, θ_r^{W}

$$\cos\theta_r^{W} = r\cos\theta_e \quad (2)$$

where r is the ratio of the area in contact with a liquid divided by the projected area, which is equal to f_1 in Eq. 1 [1]. According to Eq. 1, the smooth surface can be made more hydrophobic or oleophobic by surface roughening, regardless of θ_e. However, according to Eq. 2, θ_e has to be greater than 90° in order for a smooth surface to be more hydrophobic or oleophobic after roughening. This statement reinforces the concept of the meta-stable Cassie–Baxter model, i.e., a surface having $\theta_e < 90°$ with a liquid, when roughened, will immediately wet (Wenzel behavior) or the liquid will initially sit on top of the surface due to air pockets inside the grooves which result in a local minimum in the surface energy (meta-stable Cassie–Baxter behavior). In addition, since the surface tension of an oil such as dodecane ($\gamma = 25.4$ mJ m^{-2}) is lower than that of water ($\gamma = 72.8$ mJ m^{-2}), the θ_r^{CB} of water is higher than θ_r^{CB} of oil. Hence, according to Eq. 2, all super-oleophobic surfaces should be super-hydrophobic, but not all super-hydrophobic surfaces exhibit super-oleophobicity.

In this study, we produced a super-oleophobic surface by chemically grafting a fluoropolymer onto a non-woven, hydro-entangled nylon fabric using pulsed plasma polymerization of the monomer 1*H*,1*H*,2*H*,2*H*-perfluorodecylacrylate (PFAC8). Hydro-entangling is a process for producing a non-woven fabric by curling and entangling fiber webs using high pressure water jets [16]. Hydro-entangling technology employs neither chemical nor thermal bonding, which changes the chemical and mechanical properties of fibers after fabrication. PFAC8 is deposited in our plasma apparatus to obtain uniformly treated fabric. Indeed, previous studies have shown that grafting a PFAC8 fluoro-polymer onto surfaces using pulsed plasma polymerization is capable of conferring an exceptionally low surface energy to a range of materials [17]. The resulting material has then been modeled using a meta-stable Cassie–Baxter equation which accurately predicts the super-oleophobicity of the composite surface.

Experimental

Grafting of PFAC8 on nylon 6.6 film and hydro-entangled nylon non-woven fabric

A low surface energy chemical, PFAC8 ($C_8F_{17}CH_2CH_2OCOCH{=}CH_2$, Fluorochem, Derbyshire, UK) was deposited onto nylon 6,6 film (M_n: 12 kDa) and a non-woven nylon substrate (100 g/m^2) using pulsed plasma polymerization. The inductively coupled, cylindrical plasma reactor (10 cm diameter and 2,700 cm^3 volume) was housed in a heated Perspex chamber and connected to a two-stage Edwards rotary pump via a liquid nitrogen cold trap. Internal pressure was measured using a thermocouple pressure gauge. Prior to each experiment, the reactor was cleaned with an air plasma run at 50 Watts for 30 min. The system was pumped back down to base pressure before being raised to atmosphere to allow insertion of the material (12 cm × 8 cm). The sample was placed on a glass shelf situated within the length of the external radio frequency (RF) coil (10 turns, center-tapped, outside diameter 12 cm). An L–C matching unit was used to minimize the standing wave ratio of the transmitted power between the 13.56 MHz RF generator and the electrical discharge. An RF probe and oscilloscope were used to monitor the pulse width produced by a pulse generator. 2 mL PFAC8 was placed in a monomer tube attached to the air inlet side of the reactor and purified by freeze–thaw cycling prior to use. All connections were grease free. Whilst the reactor was pumping down, the heaters were turned on and the whole reactor heated to 30 °C. Once base pressure had been reached, the monomer was bled into the reactor through a Young's tap, and set at a pressure of approximately 1×10^{-1} mbar. After 2 min, the plasma was ignited at a peak power of 40 Watts with the pulse generator set at 40 μs on and 20 ms off. A pulsed plasma polymer deposition was carried out for 5 min using a stable pulse envelope as indicated by the oscilloscope. After the plasma treatment, the RF generator was switched off and monomer vapor allowed to purge the reactor for a further 2 min before isolating the system from the monomer vapor and pumping it down to base pressure. When base pressure had been reached, air was carefully introduced and the sample removed once the reactor was at atmospheric pressure. A schematic of the pulsed plasma polymerization apparatus is shown in Fig. 1.

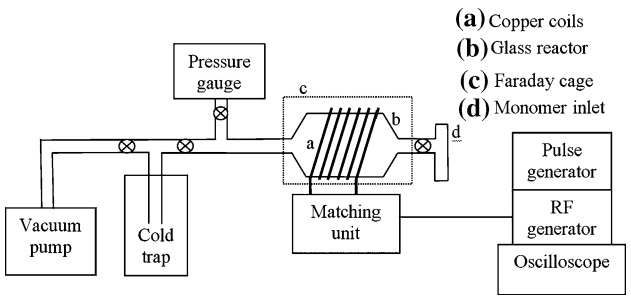

Fig. 1 Schematic representation of the pulsed plasma polymerization apparatus

Scanning electron microscopy

The rough surface of nylon non-woven fabrics were examined with a scanning electron microscope (SEM, Hitachi S-3200N) operated at 5 and 10 kV and magnifications from 25× to 150,000×. Revolution™ v1.60b24 (4pi Analysis Inc.) and Image J 1.34s (National Institute of Health) were used for image analysis of SEM images, including fiber diameters and distances between adjacent fibers.

Contact angle measurements

The contact angles of water and dodecane ($C_{12}H_{26}$, Aldrich, St. Louis, MO, USA) on the prepared surfaces were measured from sessile drops using a lab-designed goniometer at 20 °C. The range of contact angles were obtained after depositing liquids of 5, 10, 20, 50, and 100 μL each on a new spot. The roll-off angle was measured by placing a specimen on a level platform mounted on a rotation stage, Newport 495, and inclining the specimen. The images of liquid droplets on the prepared surface were obtained using a digital camera (Canon EOS EF-S-18-55IS) having an optical microscopic focusing lens (Meiji Techno EMZ-13TR). A CAHN DCA 322 dynamic contact angle analyzer was also used to measure contact angles and estimate the surface energy of plasma polymerized PFAC8 on flat glass substrates; distilled water and dodecane were used as the polar and non-polar liquid pair, respectively, to obtain geometric mean surface energy data.

Results and discussion

Chemical modification of nylon surface

Pulsed plasma polymerization of PFAC8 and subsequent characterization of the resulting polymer has been described previously [17]. The surface energy of the polymer is very low due to the long, perfluoroalkyl chains which orientate themselves normal to the solid surface and present a closely packed sheath of trifluoromethyl groups [18]. Figure 2 shows water and dodecane droplets on the nylon film. Young's contact angles of dodecane ($\theta_{\text{e-dodecane}}$) measured on the PFAC8-treated nylon film were between 78° and 81° while $\theta_{\text{e-water}}$ were between 123° and 125°.

The surface energy of the PFAC8 polymer on flat glass substrates was measured using the two liquid geometric mean method [19]. For water/dodecane, surface energies between 9.02 and 9.7 mJ m^{-2} were recorded. This compares favorably with the surface energies of the PFAC8 polymer measured on the nylon film (8.49–9.02 mJ m^{-2}).

Modeling of the super-oleophobic non-woven surface

To create a stable Cassie–Baxter surface, the Young's contact angle, θ_e, of a liquid residing on the corresponding flat surface must be greater than 90°. Despite its very low surface energy (~9 mJ m^{-2}), the PFAC8 plasma polymer cannot produce a dodecane contact angle much greater than 80°. Consequently, this surface treatment can never produce a stable Cassie–Baxter surface. Using three simultaneous equations, the surface energy of a solid may be derived from Eq. 1 from our previous research [20]:

$$\begin{aligned}\gamma_L(1+\cos\theta_e) &= \gamma_L^d(1+\cos\theta_e)+\gamma_L^p(1+\cos\theta_e)\\ &\quad+\gamma_L^H(1+\cos\theta_e)\\ &= 2\left(\sqrt{\gamma_S^d\cdot\gamma_L^d}+\sqrt{\gamma_S^p\cdot\gamma_L^p}+\sqrt{\gamma_S^H\cdot\gamma_L^H}\right)\end{aligned}$$

where γ is the surface energy; S, SL, and L are the solid–vapor, the solid–liquid, and the liquid–vapor interfaces, respectively; and the superscripts d, p, and H correspond to the London dispersion force, permanent dipole, and hydrogen bonding components of surface energy, respectively. Since the surface energies of non-polar liquids and solids such as dodecane and the PFAC8 plasma polymer are largely determined by London dispersion forces, this equation can be simplified to:

$$\gamma_L(1+\cos\theta_e) = 2\sqrt{\gamma_S^d\cdot\gamma_L^d} = 2\sqrt{\gamma_S\cdot\gamma_L} \quad (3)$$

Substituting $\gamma_L = 25.4$ mJ m^{-2} for dodecane into Eq. 3 suggests that γ_S must be smaller than 6.35 mJ m^{-2} to have θ_e greater than 90°. Despite having a Young's dodecane contact angle of less than 90°, the PFAC8 plasma-modified non-woven fabric is both super-hydrophobic and super-oleophobic, displaying apparent dodecane and water contact angles of 153°–158° and 168°–171°, respectively (Fig. 3).

In order to understand the super-oleophobicity displayed by the modified non-woven fabric, a meta-stable Cassie–Baxter model was used to help interpret the observations and predict the apparent dodecane and water contact angles using the physical parameters of the system.

A meta-stable Cassie–Baxter surface represents a locally stable Cassie–Baxter surface where a liquid initially sits on top of the surface and air pockets inside the rough structure, which results in a low surface energy for the composite surface. However, the liquid can be drawn into contact with the rough surface over time, depending upon the stability of the local energy equilibrium affected by the surface tension and volume of the liquid and the surface energy and morphology of the solid [21].

Figure 4 represents a cross-sectional view of a dodecane droplet sitting on the top layer of the hydro-entangled non-woven fabric. In Fig. 4, R is defined as the radius of a fiber, and $2d$ is the distance between two adjacent fibers. In the

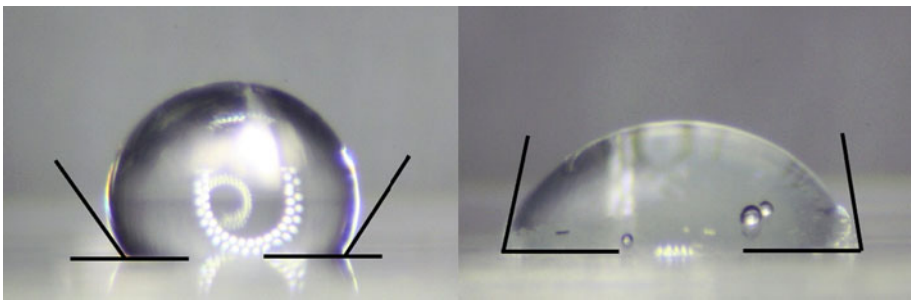

Fig. 2 Water (*left*) and dodecane (*right*) droplets on a PFAC8-grafted nylon film

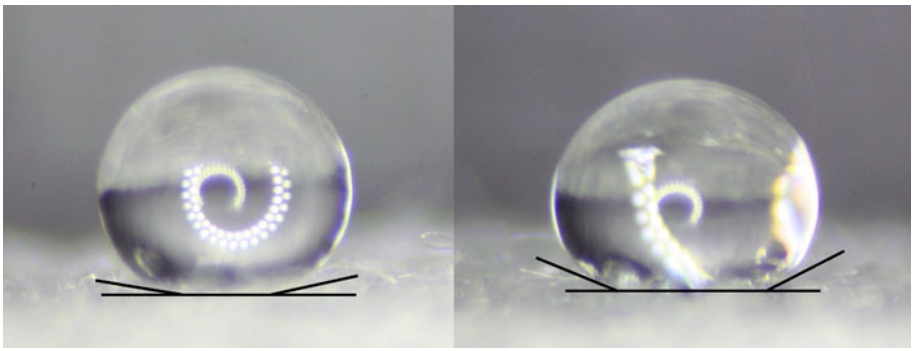

Fig. 3 Water (*left*) and dodecane (*right*) droplets on PFAC8-grafted nylon non-woven fabric

meta-stable Cassie–Baxter model, we consider two possible scenarios when $2d$ is varied: (i) $2d$ can be too large, and (ii) $2d$ can be too small. In Case (i), the robustness of the rough surface decreases and the droplet sags between two fibers, completely wetting the rough surface. However, as shown in Fig. 5, numerous fibers underneath the top layer support the droplet and prevent the surface from absorbing the liquid immediately. In Case (ii), although the roughness of fabric increases, it is difficult to obtain a morphology satisfying the meta-stable Cassie–Baxter model. This is because, when the fiber spacing is too small, there is insufficient trapped air that results in low apparent contact angles according to Eq. 1.

Firstly, we examine $2d$ for a fabric with a Wenzel roughness, r. According to Eq. 2, for a material with a smooth surface having $123° \leq \theta_{\text{e-water}} \leq 125°$ with the liquid, r must be ≥ 1.59 to make the surface super-hydrophobic. In Fig. 5, since the total area of the surface is $2(\pi R + R + d)$ while the projected area is $2(R + d)$, $r \geq 1.59$ if $2d \leq 8.65R$. As shown in Fig. 5, although the distances between two fibers of a nonwoven fabric are mostly greater than 200 μm while R is approximately 10 μm, $r \gg 1.59$. However, according to Eq. 2, a surface having $\theta_e \leq 90°$ with the liquid cannot have $\theta_r \geq 90°$, i.e., when a liquid-philic surface is roughened, $\theta_r \leq \theta_e$ and the surface can eventually absorb the liquid into the rough structure. Therefore, an advanced model which deals with not only the roughness but also the morphology of a rough surface is needed to interpret super-oleophobicity. Using the combination of the Wenzel and the Cassie–Baxter models, a meta-stable Cassie–Baxter surface having $\theta_{\text{r-dodecane}} \geq 150°$ with a liquid can be rationalized.

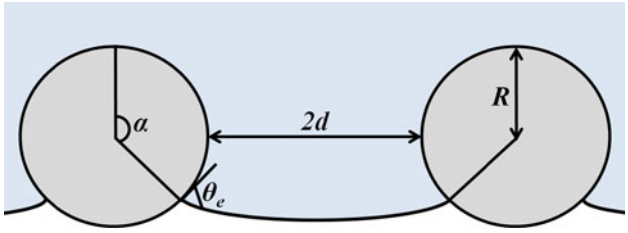

Fig. 4 A dodecane droplet sitting on the top layer of hydro-entangled non-woven fabric

By Marmur, Eq. 2 has been rewritten as follows [4]:

$$\cos\theta_r^{CB} = r_f f \cos\theta_e + f - 1 \quad (4)$$

where f is the fraction of the projected area of the solid surface in contact with the liquid and r_f is the Wenzel roughness in contact with the liquid. Before modeling a super-oleophobic surface with a hydroentangled nonwoven structure, we must prove that a non-woven structure has the potential to be a meta-stable Cassie–Baxter surface. In Fig. 4, f is given by $R \sin\alpha/(R + d)$ while r_f is $\alpha/\sin\alpha$. According to Marmur, α is equal to $\pi - \theta_e$. When $d(r_f f)/df = (\cos\sigma)^{-1}$ and $d^2(r_f f)/df^2 > 0$, local minimization of free energy can make the surface super-oleophobic.

$$\frac{d(fr_f)}{df} = \frac{d\left(\frac{Ra}{d+a}\right)}{d\left(\frac{R\sin\alpha}{d+a}\right)} = (\cos\alpha)^{-1} \quad \text{and}$$

$$\frac{d^2(fr_f)}{df} = \frac{d\left(\frac{1}{\cos\alpha}\right)}{d\left(\frac{R\sin\alpha}{d+R}\right)} > 0$$

Therefore, substituting for f and r_f into Eq. 4 results in [22]:

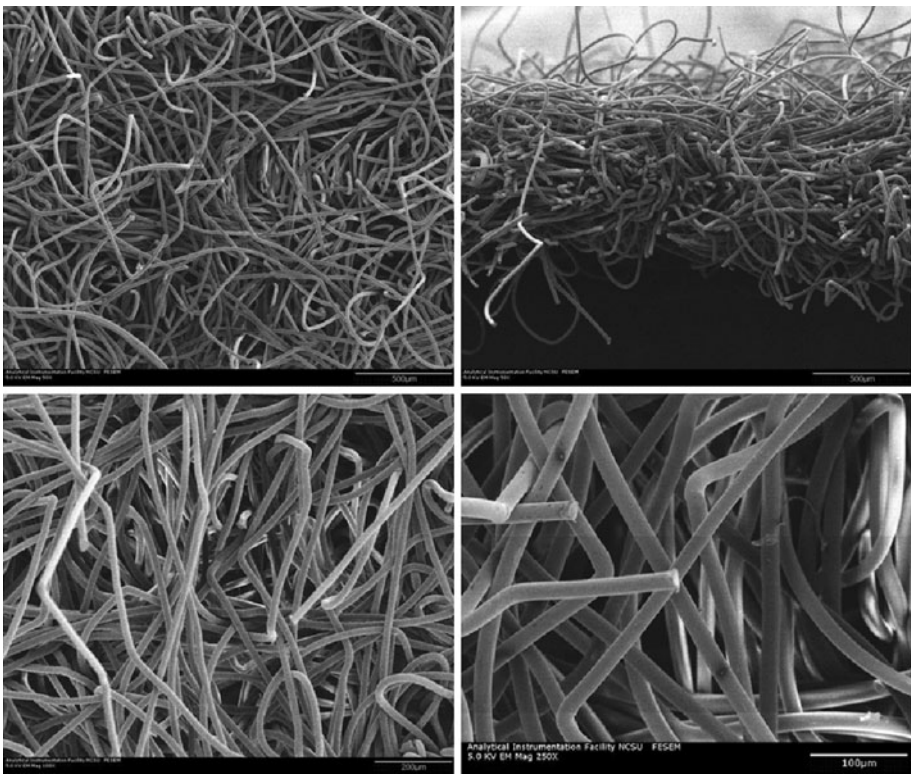

Fig. 5 SEM images of hydroentangled non-woven fabric (50×, 100×, and 250×)

$$\cos\theta_{\mathrm{r}}^{\mathrm{CB}} = \frac{R(\pi - \theta_{\mathrm{e}})}{d+R}\cos\theta_{\mathrm{e}} + \frac{R}{d+R}\sin\theta_{\mathrm{e}} - 1 \qquad (5)$$

In order to determine the average distance between the fibers within the top layer of the web, we measured f_2 based on its definition in the Cassie–Baxter model. The ratio of pores on the top layer to the projected area of the nonwoven fabric, which is regarded as f_2 in Eq. 1, was measured using Image J. This was accomplished by choosing a region in the SEM image, measuring the area of the top layer of the fabric where there were no fibers, and dividing this area by the total image area. According to the results of this analysis, the top layer of hydroentangled nonwoven fabric in Fig. 5 has a pore ratio of approximately 93%, i.e., $f_2 \approx 0.93$. Since f_2 is equal to $R\sin\theta_{\mathrm{e}}/(d+R) - 1$ in Eq. 5, $R \approx 10$ μm, and $78° \leq \theta_{\text{e-dodecane}} \leq 81°$, we calculate that $130\ \mu\mathrm{m} \leq d \leq 131\ \mu\mathrm{m}$. Then, substituting R, d, and θ_{e} to Eq. 5 results in $155° \leq \theta_{\text{r-dodecane}} \leq 156°$ and $\theta_{\text{r-water}} \approx 180°$.

The measured apparent contact angles of dodecane ($\theta_{\text{r-dodecane}}$) on a rough surface of the PFAC8-grafted nylon non-woven fabric are 153°–158° while $\theta_{\text{r-water}}$ on the same surface are 168°–171°. Good agreement between the predicted and measured contact angles is thus obtained. Both droplets sit on top of the rough surface initially, but whilst the water evaporates after 25 min, the dodecane remains for >3 h and is slowly absorbed into the nonwoven structure with a concomitant reduction in apparent contact angle.

It should also be noted that whilst droplets of water roll readily off the fabric when tilted, dodecane droplets display large advancing and receding contact angle hysteresis as they roll-off the fabric. The roll-off angles of water and dodecane were measured by placing the treated non-woven fabric on a level platform mounted on a rotation stage and inclining the fabric. The advancing and receding contact angles were measured and the roll-off angles were recorded when the drop began to move. Figures 6 and 7 show that the advancing contact angles of both water and dodecane approach 180° when the droplets begin to roll-off the surface. However, the receding contact angles are largely influenced by the surface tension of the liquid, e.g., the receding contact angle of water on the treated non-woven fabric is 145° whilst that of dodecane is 20° on the same surface. Meanwhile, the roll-off angles depend on the weight of a droplet, the surface tension of a liquid, and the receding contact angle, i.e., $mg\sin\alpha \approx \gamma_{\mathrm{L}} D(\cos\theta_{\text{Receding}} - \cos\theta_{\text{Advancing}})$ where m is the mass of the droplet, g is the gravitational acceleration, α is the roll-off angle, γ_{L} is the liquid surface tension, and D is the diameter of the wetting area [23]. Although the roll-off angle of a 50 μL droplet of water and dodecane on the treated non-woven surface is

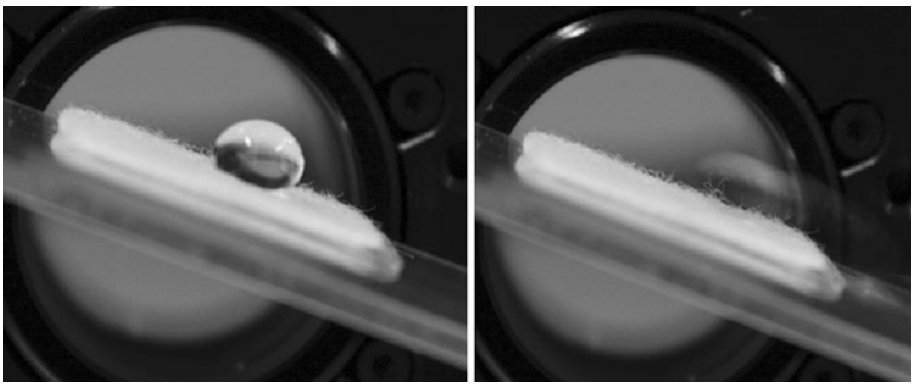

Fig. 6 Water rolling off PFAC8-grafted nylon non-woven fabric

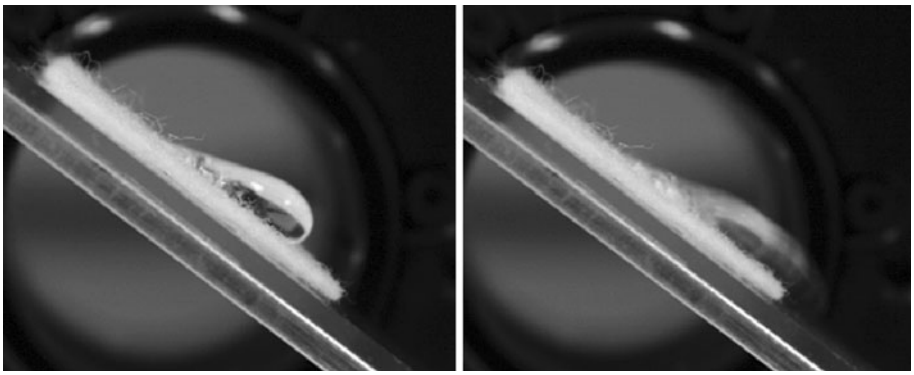

Fig. 7 Dodecane rolling off PFAC8-grafted nylon non-woven fabric

21° and 36°, respectively, as shown in Figs. 6 and 7, 5 μL droplets of water and dodecane, respectively, do not roll-off the same surface even if the fabric is inclined to 90°.

Conclusion

A super-oleophobic and super-hydrophobic material can be created by constructing a low surface energy, meta-stable Cassie–Baxter structure. A super-oleophobic and super-hydrophobic composite surface has been produced by pulsed plasma polymerization of PFAC8 onto a hydro-entangled, nylon non-woven fabric. Droplets of dodecane sit on the modified fabric with a contact angle exceeding 150°, thus satisfying the condition of super-oleophobicity. A meta-stable Cassie–Baxter model has been used to obtain theoretical, apparent contact angles for both dodecane and water on this structure; these contact angles are in good agreement with those obtained by direct measurement. In accordance with a meta-stable Cassie–Baxter surface, the dodecane droplets can penetrate the composite structure over time with a gradual drop in apparent contact angle.

Acknowledgements This material was partially sponsored by US Army Natick Soldier Research Development and Engineering Center (NSRDEC) and Air Force Research Laboratory (AFRL) under agreement number FA8650-07-1-5903. The U.S. Government is authorized to reproduce and distribute reprints for Governmental purposes notwithstanding any copyright notation thereon. We also appreciate support from the Defense Threat Reduction Agency-Joint Science and Technology Office for Chemical and Biological Defense (grant number HDTRA1-08-1-0049). We thank Nonwoven Institute (NI) for sharing hydro-entangled non-woven fabric with us.

References

1. Wenzel R (1936) Ind Eng Chem 28:988
2. Cassie A, Baxter S (1944) Trans Faraday Soc 40:546
3. Fowkes F (1963) J Phys Chem 67:2538
4. Marmur A (2003) Langmuir 19:8343
5. McHale G, Shirtcliffe N, Newton M (2004) Langmuir 20:10146
6. Lee H, Owens J (2011) J Mater Sci 46:69
7. Ohkubo Y, Tsuji I, Onishi S, Ogawa K (2010) J Mater Sci 45:4963. doi:10.1007/s10853-010-4362-2
8. Zimmermann J, Reifler F, Fortunato G, Gerhardt L, Seeger S (2008) Adv Funct Mater 18:3662
9. Rios P, Dodiuk H, Kenig S, McCarthy S, Dotan A (2008) Polym Adv Technol 19:1684
10. Levkin P, Svec F, Frechet J (2009) Adv Funct Mater 19:1993
11. Tuteja A, Choi W, Mabry J, McKinley G, Cohen R (2008) Proc Natl Acad Sci 105:18200
12. Joly L, Biben T (2009) Soft Matter 5:2549
13. Lee H, Willis C (2009) Chem Ind 21
14. Raura P, Fort J (2002) Langmuir 18:566
15. Lee H, Michielsen S (2007) J Polym Sci B 45:253
16. Butler I (1999) Nonwoven fabrics handbook. Association of the Nonwoven Fabrics, Cary, NC, USA
17. Badyal J, Brewer S, Coulson S, Willis C (2000) Chem Mater 12:2031

18. Kissa E (1984) Handbook of fiber science and technology. Marcel Dekker Inc, New York, NY, USA
19. Mittal K (1993) In contact angle wettability and adhesion. VSP BV, Zist, The Netherlands
20. Lee H (2009) J Mater Sci 44:4645. doi:10.1007/s10853-009-3711-5
21. Lee H, Owens J (2010) J Mater Sci 45:3247. doi:10.1007/s10853-010-4332-8
22. Michielsen S, Lee H (2007) Langmuir 23:6004
23. Lee H, Michielsen S (2006) J Textile Inst 97:455